Quantitative High-Field MRI of Multiple Sclerosis

David Alexander Rudko[1], Joseph Gati[1], Marcelo Kremenchutzky[2], and Ravi Menon[1]

[1]Robarts Research Institute, London, Ontario, Canada, [2]Clinical Neurological Sciences, University of Western Ontario, London, Ontario, Canada

Introduction: Conventional magnetic resonance imaging (MRI) measures of multiple sclerosis (MS) disease status (number and location of lesions in white matter) have not correlated well with clinical symptoms and have not demonstrated significant predictive power for determining disease progression[1,2]. Neuropathological studies have identified the following hallmark features as highly linked to MS etiology and neurodegeneration: (i) *changes in the chemical composition of myelin* and (ii) *accumulation of iron in brain regions affected by MS* [3]. Standard MRI at 1.5 Tesla (T) and 3 T is unable to adequately visualize this subtle neurodegeneration. In this study, we use high-resolution magnetic susceptibility-based MRI at 7 T to identify regions of increased iron deposition and decreased myelination in MS patients compared to healthy, age-matched control subjects.

Methods: Informed consent was obtained from 14 MS patients and 7 healthy volunteers for this study which was approved by the Human Subjects Research Ethics Board of the University of Western Ontario. Imaging experiments were performed on a 7 T neuroimaging scanner using either 16 or 23 channel receive coils. For each imaging session, three acquisitions were performed: (i) a 3D multi-echo gradient imaging sequence ($0.5 \times 0.5 \times 1.25$ mm^3 resolution) to obtain susceptibility-weighted images (ii) a T_2-weighted, magnetization-prepared, fluid-attenuated inversion recovery (MP-FLAIR) sequence ($1.0 \times 1.0 \times 1.0$ mm^3 resolution) for lesion delineation and (iii) a T_1-weighted, MPRAGE acquisition ($1.0 \times 1.0 \times 1.0$ mm^3 resolution) for anatomical reference and use in tissue segmentation. Manual segmentation of hyperintensities on MP-FLAIR images was used to identify lesions. Additionally, from the gradient echo data, susceptibility-weighted (SWI), R_2^*, local frequency shift (LFS) and quantitative susceptibility (QS) maps were reconstructed. Quantitative maps for all the subjects were non-linearly registered to the MNI-T_{1w}-1mm template using the FSL FNIRT[4] tool and group-averaged R_2^*, LFS and QS maps in the MNI-T_{1w}-1mm space were computed for MS patients and healthy controls.

Basal Ganglia Structure	Patients	Controls	p-value
Caudate	45.05 ± 0.50	44.15 ± 0.26	0.04
Putamen	47.27 ± 0.60	46.31 ± 0.35	0.07
Pallidum	91.18 ± 1.45	88.54 ± 1.22	0.02
Thalamus	41.04 ± 0.61	39.31 ± 0.42	0.007

Table1: Comparison of mean R_2^* in basal ganglia structures of MS patients to R_2^* of age-matched controls.

Results: Table 1 compares the R_2^* values in basal ganglia structures of MS patients and controls. Statistically significant differences were computed in the caudate nucleus, pallidum and thalamus, while the putamen showed a trend towards significance ($p = 0.07$). A total of 108 lesions were segmented manually by identifying hyperintensities on the 7 T MP-FLAIR images. Of those 108 lesions, 102 were visible on T_{1w} images, 56 were visible on R_2^* maps and 21 were visible on both the LFS and QS maps. The mean R_2^* value in white matter lesions was 27.18 ± 1.13 s^{-1} while the mean R_2^* in surrounding normal-appearing white matter (NAWM) was significantly higher ($p < 0.01$) with a value of 33.18 ± 0.60 s^{-1}. The right-most column of Figure 1 shows quantitative difference maps comparing R_2^*, LFS and QSM in MS patients to age-matched controls. Consistent differences in R_2^* and QS maps were observed in the basal ganglia structures and the optic radiations. The group-averaged maps of the thalamus delineate MS relevant thalamic sub-structures (the lateral nuclei, the medial nuclei and the pulvinar).

Conclusion: This study employed high-field (7 T) MR imaging in conjunction with advanced post-processing techniques to evaluate iron and myelin whole-brain changes in MS patients compared to healthy, age-matched controls. All the quantitative maps evaluated in this study showed evidence of increased iron deposition in basal ganglia structures in MS patients. QS maps are preferentially sensitive to increased iron in the basal ganglia as illustrated in the right-most column of Figure 1. Calculation of group-averaged maps also allowed comparison of R_2^*, LFS and QS values in three MS relevant sub-structures of the thalamus. The pulvinar nucleus consistently displayed the most significant changes in R_2^*, LFS and QS maps in MS patients compared to healthy age-matched controls.

References: 1) Moral et al. Archives of Neurology 2009; 66: 1345 – 1352. (2) Rudick et al. Journal of Neurological Sciences 2009; 282 : 106 - 111 (3) Haacke et al. JMRI 2009; 29(3) : 537 -544. (4) Andresson et al. Human Brain Mapping 2008 ; Poster #496.
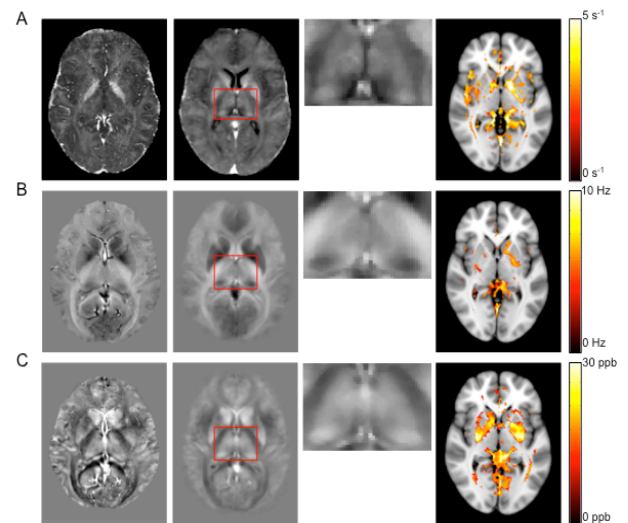
Figure 1. Comparison of (A) R_2^*, (B) LFS and (C) QS maps for a single subject (left-most column), the group-averaged template, an enlarged view of the thalamus and quantitative difference maps between group-averaged MS patients and controls (right-most column). The quantitative difference maps are given for a single slice through the basal ganglia structures.